

# Manganese-Catalyzed Surface Growth of Single-Walled Carbon Nanotubes with High Efficiency

Bilu Liu, Wencai Ren,\* Libo Gao, Shisheng Li, Qingfeng Liu, Chuanbin Jiang, and Hui-Ming Cheng\*

Shenyang National Laboratory for Materials Science, Institute of Metal Research, Chinese Academy of Sciences, Shenyang 110016, People's Republic of China

Received: July 9, 2008; Revised Manuscript Received: September 29, 2008

We demonstrate that manganese (Mn) can catalyze the growth of single-walled carbon nanotubes (SWNTs) with high efficiency via a chemical vapor deposition process. Dense and uniform SWNT films with high quality were obtained by using a Mn catalyst, as characterized by scanning electron microscopy, Raman spectroscopy, atomic force microscopy, and transmission electron microscopy. Moreover, we found that the surface property of the substrate plays a critical role in the growth efficiency of SWNTs. By deposition of a thin oxide layer ( $\text{SiO}_2$  or  $\text{Al}_2\text{O}_3$ ) on the top of a  $\text{SiO}_2/\text{Si}$  substrate, the growth efficiency of SWNTs was dramatically improved. The successful growth of SWNTs by Mn catalyst provides new experimental information for understanding the growth mechanism of SWNTs, which may be helpful for their controllable synthesis.

## Introduction

Because of the unique structure and excellent properties, carbon nanotubes (CNTs), especially single-walled carbon nanotubes (SWNTs), have attracted a great deal of attention as model systems for nanoscience and for various applications.<sup>1</sup> Both theoretical calculations and experimental results suggest that a SWNT can be either metallic or semiconducting, depending on its diameter and chiral angle, i.e.,  $(n,m)$  index.<sup>2</sup> Therefore, controllable synthesis of SWNTs is of great importance for their practical applications, in particular in electronic devices.<sup>1</sup>

Recent experimental<sup>3–5</sup> and theoretical<sup>6,7</sup> investigations show that the controllable synthesis of SWNTs can be realized in some degree by careful selection of catalyst elements<sup>4,6,7</sup> or their alloys.<sup>3,5,6</sup> For instance, high chiral angle (6,5) and (7,5) SWNTs, occupying a total of 57% of semiconducting SWNTs, can be obtained by the use of Co–Mo alloy catalyst;<sup>3</sup> while (6,5) or (8,4)-dominant SWNTs can be selectively synthesized with Fe–Ru alloy catalyst.<sup>5</sup> By using first-principles calculations, Yazyev et al. suggested that relative stability of SWNT nucleus varies significantly with different metals as well as SWNT types. This reveals that the chirality distributions of the as-synthesized SWNTs can be controlled by using different catalyst elements.<sup>7</sup> The calculated results reported by Ding et al. using density functional theory (DFT) also indicate that by adjustment of the chemical composition of catalyst particles the carbon–metal adhesion strength would be systematically changed. This influences the chirality of SWNT products, for instance, zigzag-predominated SWNTs can be fulfilled by using special designed metals or their alloys.<sup>6</sup> Therefore, exploration of the possibility of growing SWNTs using different catalyst systems is of great importance both for their controllable synthesis as well as for understanding of their growth mechanism. Besides the commonly used catalysts, iron-group metals (Fe, Co, Ni) and their alloys<sup>8–11</sup> for the growth of SWNTs, recent experimental results

have demonstrated that inert coinage metals (Cu, Ag, Au),<sup>4,12,13</sup> heavy late-transition metals (Pd, Pt),<sup>12</sup> Re<sup>14</sup> and even semiconductor nanoparticles (Si, SiC and Ge)<sup>15</sup> can also be used for the catalyzed growth of SWNTs in the chemical vapor deposition (CVD) process. Moreover, Zhou et al. found that a high percentage of metallic SWNTs were obtained using Cu catalyst.<sup>4</sup>

Manganese (Mn), located near iron in the periodic table of elements, is widely used as a cocatalyst in various chemical reactions, such as Rh- or Fe-catalyzed Fischer–Tropsch synthesis<sup>16,17</sup> and *n*-butane isomerization reaction.<sup>18</sup> The addition of Mn is considered to be able to attract oxygen from CO and facilitate the dissociation of CO in the Fischer–Tropsch synthesis process<sup>16</sup> and can influence the dispersion of Fe catalyst in the *n*-butane conversion reaction.<sup>18</sup> However, Mn is rarely used as catalyst for CNT synthesis. Moreover, it has been predicted, based on carbon–metal binary phase diagrams, that Mn is not a suitable catalyst for CNT growth because of kinetic reasons of carbon diffusion and multiple carbides formation.<sup>19</sup>

In this contribution, we demonstrate that Mn can be used as catalyst for efficient growth of SWNTs by using a CVD method. Moreover, it was found that the growth efficiency can be dramatically improved by changing the substrate's surface property. Dense and uniform high-quality SWNT thin films were obtained on the  $\text{SiO}_2/\text{Si}$  substrate capped by an additional 10-nm-thick  $\text{SiO}_2$  or  $\text{Al}_2\text{O}_3$  layer.

## Experimental Section

**A. SWNT Synthesis.** Ten mM ethanol solution of manganese (II) chloride ( $\text{MnCl}_2$ ) was used as catalyst precursor. Two kinds of substrates were employed in our experiments. One is silicon wafer covered with 1- $\mu\text{m}$ -thick thermally oxidized  $\text{SiO}_2$  at 1000 °C (type 1). The other substrate (type 2) was prepared by depositing an additional 10-nm-thick  $\text{SiO}_2$  or  $\text{Al}_2\text{O}_3$  layer on type 1 substrate with a high deposition rate of 1 Å/s using an ion-beam assisted deposition technique (Gatan Model 682 precision etching coating system) at room temperature. For the loading of Mn catalyst on the substrate, we simply immersed

\* To whom correspondence should be addressed. E-mail: cheng@imr.ac.cn (H-M.C.); wren@imr.ac.cn (W.C.R).

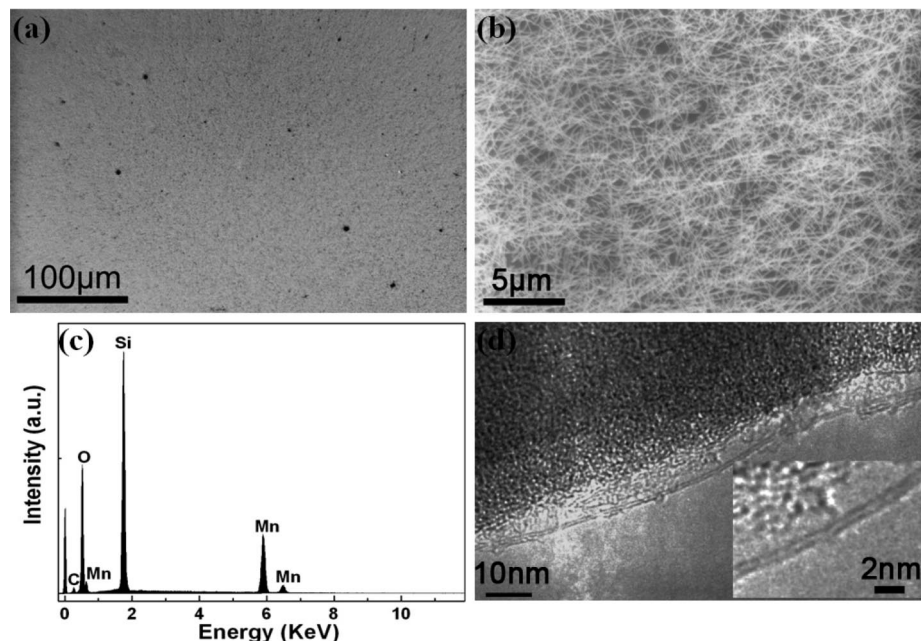


**Figure 1.** (a) Low-magnification and (b) high-magnification SEM images of the as-grown dense and uniform SWNT films. The SEM images were obtained at a low electron accelerating voltage of 1 kV, because surface grown SWNTs can be seen at low voltage<sup>4,8–11,13,21</sup> due to enhanced secondary electron emission from the nearby insulator surface.<sup>20</sup> (c) EDS spectrum of the substrate after SWNT growth. (d) HRTEM image of an individual SWNT, and the inset is its enlarged image.

the substrates into MnCl<sub>2</sub> ethanol solution for 10 s followed by blow-drying with high-purity Ar gas.

The SWNT synthesis was performed in a Lindberg/Blue M tube furnace equipped with a 25 mm diameter quartz tube. To obtain a stable gas flow, a small quartz tube with a diameter of 10 mm was employed to load the substrate,<sup>11</sup> which was then inserted into the 25 mm reaction tube. Mn catalyst precursor was first calcined with 50 standard cubic centimeter per minute (sccm) of N<sub>2</sub> + O<sub>2</sub> (4:1, v:v) gas mixture for 10 min at 850 °C and then reduced with 100 sccm Ar + 200 sccm H<sub>2</sub> for 10 min. After these catalyst pretreatment processes, the furnace was heated to 900 °C under Ar + H<sub>2</sub> gas mixture and the reaction was ignited by adding 500 sccm of CH<sub>4</sub> as carbon source. Typically, the growth process sustained for 20 min, and was then terminated by switching off the CH<sub>4</sub> gas. After growth, the furnace was cooled down naturally to room temperature under the protection of Ar + H<sub>2</sub> gas mixture.

**B. SWNT Characterization.** The as-grown SWNTs were characterized by scanning electron microscopy (SEM, LEO SUPRA 35 and Nova NanoSEM 430, operated at 1 kV for imaging<sup>20</sup> and 20 kV for energy dispersive spectroscopy (EDS)), atomic force microscopy (AFM, multimode NanoScope IIIa, Veeco, operated in tapping mode), Raman spectroscopy (Jobin Yvon HR800, excited by 632.8-nm He–Ne laser with laser spot size of  $\sim 1 \mu\text{m}^2$ ), and high-resolution transmission electron microscopy (HRTEM, JEOL 2010, operated at 200 kV and Tecnai F30, operated at 300 kV).

## Results and Discussion

Figure 1 exhibits the typical results of the as-grown SWNTs on type 2 substrate (with a 10-nm-thick SiO<sub>2</sub> layer coated on type 1 substrate). We can see clearly from parts a and b of Figure 1 that a dense and uniform SWNT film is obtained by using Mn as catalyst. Such large-area uniform SWNT films show attractive applications in SWNT based thin-film transistors.<sup>21</sup> The black spots in Figure 1a are bared substrate without SWNTs grown on it, as proven by high-magnification SEM images

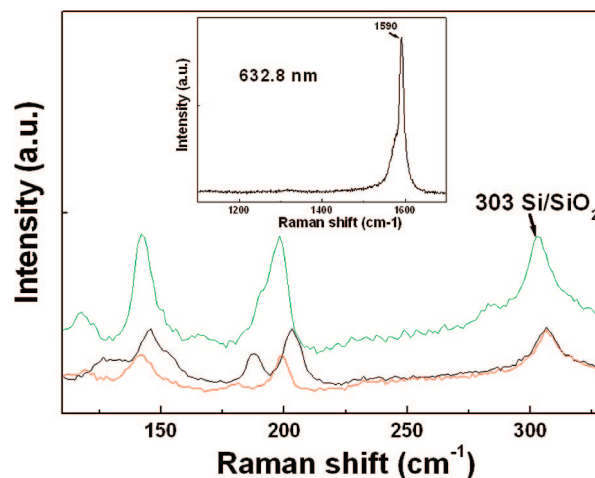


**Figure 2.** Raman spectra of SWNTs from three different positions of the same sample in Figure 1. The peaks at  $\sim 303 \text{ cm}^{-1}$  are from SiO<sub>2</sub>/Si substrate and used for the calibration of SWNT Raman spectra. The inset shows typical G band and D band feature of the sample.

(Figure 1b). Figure 1c is a typical EDS spectrum of the substrate after SWNT growth, showing the presence of Mn. It is needed to point out that Fe, Co, Ni, and any other metal elements were not found in the sample, indicating that it is Mn that acts as catalyst in the growth process. We also conducted TEM to investigate the detailed structure of SWNTs. To retain the original morphology of the as-grown SWNTs, we directly scratched the substrate surface with a TEM grid for sample preparation. Though it is very difficult to observe SWNTs from surface growth by HRTEM, careful observations reveal that the as-grown SWNTs possess a high-quality and clean surface, as shown in Figure 1d. Moreover, most SWNTs are found to be individual ones, while very small bundles were occasionally seen in our HRTEM observations.

Raman spectroscopy provides a powerful tool to characterize the diameter and quality of SWNTs. Figure 2 shows Raman spectra of three different positions of the same sample in Figure

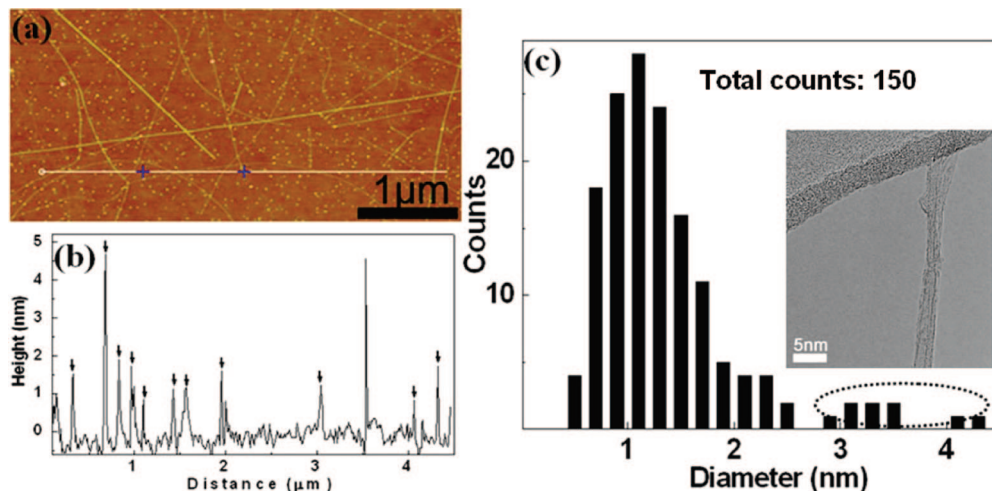


**Figure 3.** (a) A representative AFM image of SWNTs at a low-density area. (b) The corresponding topographic height profile along the white line in part a, with the SWNT heights indicated by black arrows. (c) Diameter distribution of the SWNTs obtained from AFM measurements of 150 SWNTs, with the dotted ellipse indicating SWNT bundles. Inset: HRTEM image of a small SWNT bundle ( $\sim 3$  nm) occasionally observed in the sample.

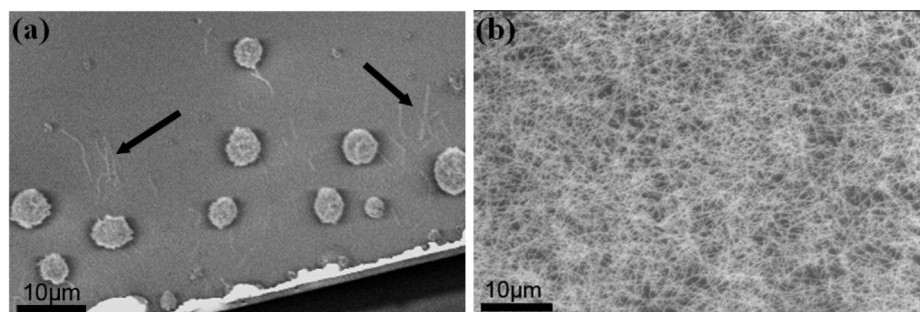


**Figure 4.** (a) Short and sparse SWNTs grown on the type 1 substrate, denoted by black arrows. (b) Dense and uniform SWNT thin film grown on the type 2 substrate. All the other growth parameters kept the same in our experiments except for the substrates.

1, and several radial breathing mode (RBM) signals were found from one laser spot ( $\sim 1 \mu\text{m}^2$ ). The RBM frequencies are in the range of  $120\text{--}310 \text{ cm}^{-1}$ , which suggests that the diameter of SWNTs in our sample is distributed from 0.8 to 2.1 nm, according to the formula  $d_t = 248/\omega_{\text{RBM}}$ .<sup>22</sup> We should point out that large SWNTs ( $> 2.5$  nm) can not be probed by Raman spectroscopy due to their very small Raman cross sections. It is known that the D band is related to vacancies, impurities, or other symmetry-breaking defects in SWNTs. The presence of RBM and the low intensity ratio ( $\sim 0.04$ ) of the disorder-induced D band to tangential G band (shown in inset of Figure 2) further prove the high quality of SWNTs obtained.

AFM was also employed to investigate the diameter of SWNTs. Because the crossing of nanotubes has a great influence on the real height evaluation of SWNTs, we intentionally selected the areas with relatively low SWNT density during the AFM measurements. Figure 3a presents a representative AFM image of such a low-density area. The corresponding topography height profile along the white line in Figure 3a is shown in Figure 3b. On the basis of AFM measurements on 150 tubes, we obtained the diameter distribution of the SWNTs, as shown in Figure 3c. The SWNTs have a relatively small average diameter of 1.1 nm, with most of them having a diameter less than 2.0 nm (131 tubes in 150, i.e., 87%). This result is in agreement with that obtained by Raman spectroscopy. The topographic height larger than 3.0 nm shown in parts b and c of Figure 3 is suggested to be related to small SWNT bundles (inset of Figure 3c), since multiwalled carbon nanotubes (MWNTs) were not found from the HRTEM observations.

Our results also demonstrate that a small difference in substrates can lead to a remarkable difference on the growth efficiency of SWNTs. Type 1 substrate is a single crystal silicon wafer covered by  $1\text{-}\mu\text{m}$ -thick thermally oxidized  $\text{SiO}_2$  and was widely employed in the surface growth of SWNTs.<sup>4,8–11</sup> By using this kind of substrate, we found that only very short ( $< 10 \mu\text{m}$ ) and sparse SWNTs were obtained with Mn catalyst, as indicated by the black arrows in Figure 4a. However, on type 2 substrate, which was obtained after depositing a 10-nm  $\text{SiO}_2$  layer on type 1 substrate, it is surprising to find that the growth efficiency of SWNTs was dramatically improved (Figure 4b). It is important to note that the only difference for the growth of these two samples is the substrate employed, with all other growth parameters remaining the same. Another distinct difference between these two samples observed from parts a and b of Figure 4 is that there are many big catalyst islands, several micrometers in size, on the type 1 substrate, while no catalyst island was found on the type 2 substrate. These results indicate that Mn catalyst particles can easily aggregate into big particles or islands that are no longer suitable for the growth of SWNTs on the type 1 substrate, resulting in very poor growth efficiency.

Delzeit et al. reported that depositing a 1–20-nm thin metal film (such as Ir, Al, Nb, or Ti) under the catalyst Fe film can improve the density of as-grown SWNTs on substrate, and they attributed this to an increase of the surface roughness of the substrate.<sup>23</sup> To elucidate the difference of SWNT growth on different substrates in our experiments, we used AFM to investigate the surface roughness of these two kinds of substrates. The three-dimensional (3-D) AFM images are shown



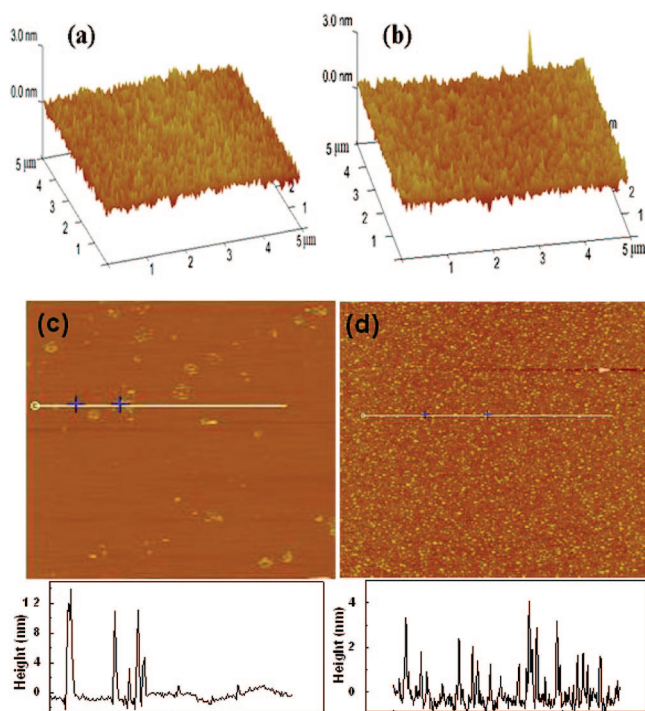


**Figure 5.** 3-D AFM images of a  $5 \times 5 \mu\text{m}^2$  area on (a) type 1 substrate and (b) type 2 substrate, showing a similar surface roughness. (c), (d)  $5 \times 5 \mu\text{m}^2$  AFM images and the corresponding height cross-sections of catalyst particles on type 1 (c) and type 2 (d) substrates. The catalysts were first calcined in  $\text{N}_2 + \text{O}_2$ , followed by reduction in  $\text{Ar} + \text{H}_2$ , just prior to  $\text{CH}_4$  exposure.

in parts a and b of Figure 5. We do not find any notable difference in surface roughness between these two kinds of substrates, and both of them have a roughness of  $\sim 1\text{--}2$  nm. Thus, we believe that there is no direct relationship between SWNT yield and the substrate roughness, and there should exist other mechanism responsible for this remarkable difference in growth efficiency.

Despite the similar surface roughness, the  $\text{SiO}_2$  upper layer on type 1 substrate, which was grown by thermal oxidation of silicon at high temperature, is a dense and uniform film.<sup>24</sup> But the  $\text{SiO}_2$  layer on type 2 substrate was prepared by sputtering technique at room temperature. Brunet-Bruneau et al. investigated the properties of evaporated  $\text{SiO}_2$  films by using infrared ellipsometry and found that such a deposited  $\text{SiO}_2$  film had a complex structure with lower density (even lower than fused silica) and possessed high pore volume fraction.<sup>25,26</sup> The newly deposited  $\text{SiO}_2$  film also undergoes a loose contact at the

interface and exhibits inhomogeneous structure.<sup>27</sup> Therefore, we speculate that the newly deposited  $\text{SiO}_2$  film (type 2 substrate) is in some degree similar to the porous catalyst support materials (such as porous  $\text{SiO}_2$ ,  $\text{Al}_2\text{O}_3$ , and  $\text{MgO}$ ) commonly used for bulk growth of SWNTs.<sup>3,5,28</sup> Such a loose and porous  $\text{SiO}_2$  layer can protect catalyst particles from aggregation and provide more suitable catalyst nanoparticles for SWNT growth.<sup>23,28</sup> This point can be confirmed by the AFM results, as shown in parts c and d of Figure 5. The catalyst particles on type 1 substrate (Figure 5c) typically aggregate into large island structures while they are well scattered in type 2 substrate (Figure 5d). The average size derived from Figure 5d is 3.1 nm, which is suitable for SWNT growth. As a result, SWNT can grow more efficiently on the type 2 substrate than on the type 1 substrate.

To demonstrate the applicability of Mn catalyst as well as highlight the importance of deposited film, we performed the growth of SWNTs using Mn catalyst on 10 nm  $\text{Al}_2\text{O}_3$  layer-coated type 1 substrate (the  $\text{Al}_2\text{O}_3$  layer was deposited in a way similar with that of  $\text{SiO}_2$  upper layer on type 2 substrate and the growth parameters were kept the same). The SEM image (Figure 6a) and corresponding Raman spectrum (Figure 6b) demonstrate the high-efficiency growth of SWNTs on the 10 nm  $\text{Al}_2\text{O}_3$  coated type 1 substrate. We can see a thin SWNT film with much higher density was obtained on 10-nm  $\text{Al}_2\text{O}_3$ -coated type 1 substrate than that of type 1 substrate (Figure 4a). We believe that this simple film deposition method can also be applied to improve the efficiency in surface growth of SWNTs using other catalysts, such as commonly used Fe, Co, and Ni.

From the C–Mn binary phase diagram, C atoms have a solubility of  $\sim 0.5$  % in C–Mn solid solution in the growth temperature (900 °C).<sup>29</sup> Thus, C atoms can diffuse in a significant amount into the nanoscaled Mn particles to catalyze the growth of SWNTs through a traditional vapor–liquid–solid process.

Structure-selective synthesis of SWNTs is of critical importance while the abortive choice of catalysts is one of the feasible strategies toward such goal.<sup>3–7,13</sup> First, both the interaction between the SWNT nucleus and metallic catalysts and the relative stability of SWNT nucleus vary remarkably with metal species as well as SWNT types.<sup>7</sup> Second, whether a SWNT nucleus can grow into a SWNT or not depends on the competing of carbon–metal adhesion strength against cap formation energy (the carbon–metal adhesion strength must be stronger than the cap formation energy to sustain SWNT growth), while their relative strength can be modified by varying metal species and SWNT chiralities.<sup>6</sup> In addition, the difference of interatomic distance for different catalysts can affect the dissociation of

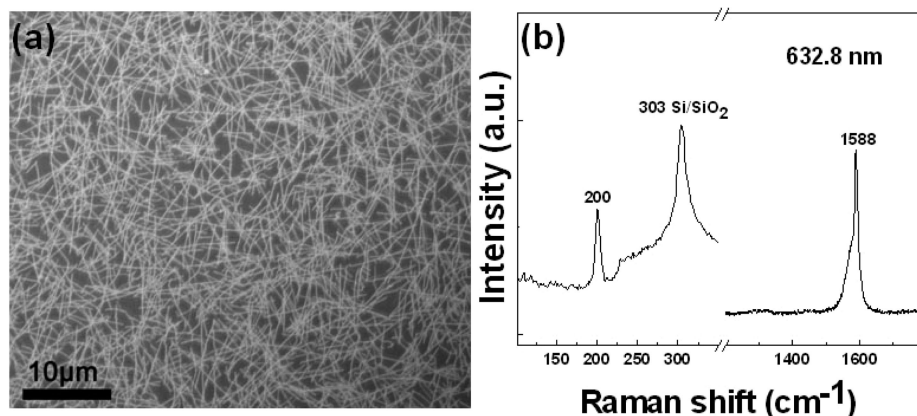


**Figure 6.** SEM image (a) and Raman spectrum (b) of the SWNTs grown on a 10-nm  $\text{Al}_2\text{O}_3$ -coated type 1 substrate.

hydrocarbon, then carbon feeding rate, and consequently the growth behavior of SWNTs. These theoretical works reveal that the catalyst type is one of the important parameters to determine the structure of grown SWNTs. Therefore, we believe that the growth behavior and the resulting structural characteristics of SWNTs (such as the metallic to semiconducting ratio of SWNTs and their chirality distribution) prepared by Mn catalyst may be different from other catalysts or their alloys. Further understanding on the Mn-catalyzed growth mechanism and detailed structural analysis of SWNTs compared with SWNTs catalyzed from other metals (such as Fe and Co), using photoluminescence excitation/emission<sup>1,3,5</sup> and optical adsorption spectra,<sup>1,5</sup> are very important.

## Conclusions

We demonstrate that Mn, a previously rarely used catalyst, can be used for the high-efficiency growth of SWNTs. It is also found that the surface property of the substrate plays a critical role in the growth efficiency of SWNTs. By deposition of a 10-nm-thick oxide layer (SiO<sub>2</sub> or Al<sub>2</sub>O<sub>3</sub>) on a thermally oxidized Si substrate, the SWNT growth efficiency can be greatly improved and dense and uniform SWNT films with high quality were obtained. The successful growth of SWNTs by Mn catalyst provides new information for the understanding of the growth mechanism of SWNTs and will be helpful for their controllable synthesis.

Additional remark: During the preparation of this manuscript, we became aware of a related work on growth of SWNTs by using Mn and other metal catalysts from Prof. Liu's group in Duke University was just published.<sup>30</sup>

**Acknowledgment.** The authors thank Mr. Da-Wei Wang and Qing-Liang Wang for helpful discussion. We acknowledge support by MOST of China (No. 2006CB932701 and No. 20089FA51400), NSFC (No. 90606008 and No. 50702063), and CAS (No. KJCX2-YW-M01).

## References and Notes

- (1) Jorio, A.; Dresselhaus, G.; Dresselhaus, M. S. *Carbon Nanotubes: Vol. 111 of Topics in Applied Physics*; Springer-Verlag: Berlin/Heidelberg, 2008.
- (2) Saito, R.; Dresselhaus, G.; Dresselhaus, M. S. *Physical Properties of Carbon Nanotubes*; Imperial College Press: London, UK, 1998.
- (3) Bachilo, S. M.; Balzano, L.; Herrera, J. E.; Pompeo, F.; Resasco, D. E.; Weisman, R. B. *J. Am. Chem. Soc.* **2003**, *125*, 11186.

- (4) Zhou, W. W.; Han, Z. Y.; Wang, J. Y.; Zhang, Y.; Jin, Z.; Sun, X.; Zhang, Y. W.; Yan, C. H.; Li, Y. *Nano Lett.* **2006**, *6*, 2987.
- (5) Li, X. L.; Tu, X. M.; Zoric, S.; Welscher, K.; Seo, W. S.; Zhao, W.; Dai, H. J. *J. Am. Chem. Soc.* **2007**, *129*, 15770.
- (6) Ding, F.; Larsson, P.; Larsson, J. A.; Ahuja, R.; Duan, H. M.; Rosen, A.; Bolton, K. *Nano Lett.* **2008**, *8*, 463.
- (7) Yazyev, O. V.; Pasquarello, A. *Phys. Rev. Lett.* **2008**, 100.
- (8) Huang, S. M.; Cai, X. Y.; Liu, J. *J. Am. Chem. Soc.* **2003**, *125*, 5636.
- (9) Zheng, L. X.; O'Connell, M. J.; Doorn, S. K.; Liao, X. Z.; Zhao, Y. H.; Akhadow, E. A.; Hoffbauer, M. A.; Roop, B. J.; Jia, Q. X.; Dye, R. C.; Peterson, D. E.; Huang, S. M.; Liu, J.; Zhu, Y. T. *Nat. Mater.* **2004**, *3*, 673.
- (10) Huang, L. M.; White, B.; Sfeir, M. Y.; Huang, M. Y.; Huang, H. X.; Wind, S.; Hone, J.; O'Brien, S. *J. Phys. Chem. B* **2006**, *110*, 11103.
- (11) Hong, B. H.; Lee, J. Y.; Beetz, T.; Zhu, Y. M.; Kim, P.; Kim, K. S. *J. Am. Chem. Soc.* **2005**, *127*, 15336.
- (12) Takagi, D.; Homma, Y.; Hibino, H.; Suzuki, S.; Kobayashi, Y. *Nano Lett.* **2006**, *6*, 2642.
- (13) Bhaviripudi, S.; Mile, E.; Steiner, S. A.; Zare, A. T.; Dresselhaus, M. S.; Belcher, A. M.; Kong, J. *J. Am. Chem. Soc.* **2007**, *129*, 1516.
- (14) Ritschel, M.; Leonhardt, A.; Elefant, D.; Oswald, S.; Buchner, B. *J. Phys. Chem. C* **2007**, *111*, 8414.
- (15) Takagi, D.; Hibino, H.; Suzuki, S.; Kobayashi, Y.; Homma, Y. *Nano Lett.* **2007**, *7*, 2272.
- (16) Pan, X. L.; Fan, Z. L.; Chen, W.; Ding, Y. J.; Luo, H. Y.; Bao, X. H. *Nat. Mater.* **2007**, *6*, 507.
- (17) Zhang, C. H.; Yang, Y.; Teng, B. T.; Li, T. Z.; Zheng, H. Y.; Xiang, H. W.; Li, Y. W. *J. Catal.* **2006**, *237*, 405.
- (18) Garcia, E. A.; Rueda, E. H.; Rouco, A. J. *Appl. Catal., A* **2001**, *210*, 363.
- (19) Deck, C. P.; Vecchio, K. *Carbon* **2006**, *44*, 267.
- (20) Homma, Y.; Suzuki, S.; Kobayashi, Y.; Nagase, M.; Takagi, D. *Appl. Phys. Lett.* **2004**, *84*, 1750.
- (21) Kocabas, C.; Shim, M.; Rogers, J. A. *J. Am. Chem. Soc.* **2006**, *128*, 4540.
- (22) Jorio, A.; Saito, R.; Hafner, J. H.; Lieber, C. M.; Hunter, M.; McClure, T.; Dresselhaus, G.; Dresselhaus, M. S. *Phys. Rev. Lett.* **2001**, *86*, 1118.
- (23) Delzeit, L.; Chen, B.; Cassell, A.; Stevens, R.; Nguyen, C.; Meyyappan, M. *Chem. Phys. Lett.* **2001**, *348*, 368.
- (24) Marathe, V. G.; Chandani, N.; DasGupta, N. *Thin Solid Films* **2006**, *504*, 126.
- (25) BrunetBruneau, A.; Rivory, J.; Rafin, B.; Robic, J. Y.; Chaton, P. *J. Appl. Phys.* **1997**, *82*, 1330.
- (26) Lee, W. Y.; Lin, H.; Gu, L.; Leou, K. C.; Tsai, C. H. *Diamond Relat. Mater.* **2008**, *17*, 66.
- (27) Li, B. Q.; Fujimoto, T.; Kojima, I. *J. Phys. D: Appl. Phys.* **1999**, *32*, 1287.
- (28) Ward, J. W.; Wei, B. Q.; Ajayan, P. M. *Chem. Phys. Lett.* **2003**, *376*, 717.
- (29) Metallography, structures, and phase diagrams; Metals Park, OH: American Society for Metals, 1973.
- (30) Yuan, D. N.; Ding, L.; Chu, H. B.; Feng, Y. Y.; McNicholas, T. P.; Liu, J. *Nano Lett.* **2008**, *8*, 2576.

JP8060587